Temporal–Spatial Monitoring of an Extreme Precipitation Event: Determining Simultaneously the Time Period It Lasts and the Geographic Region It Affects

ER LU AND WEI ZHAO

Key Laboratory of Meteorological Disaster, Ministry of Education, and Joint International Research Laboratory of Climate and Environment Change, and Collaborative Innovation Center on Forecast and Evaluation of Meteorological Disasters, Nanjing University of Information Science and Technology, Nanjing, Jiangsu, China

XUKAI ZOU AND DIANXIU YE

National Climate Center, CMA, Beijing, China

CHUNYU ZHAO

Shenyang Regional Climate Center, Shenyang, Liaoning, China

QIANG ZHANG

National Climate Center, CMA, Beijing, China

(Manuscript received 21 February 2017, in final form 9 May 2017)

ABSTRACT

A method is developed in this study to monitor and detect extreme precipitation events. For a rainfall event to be severe, it should last for a long period and affect a wide region while maintaining a strong intensity. However, if the duration is inappropriately taken as too long and the region is inappropriately taken as too wide, then the averaged intensity might be too weak. There should be a balance among the three quantities. Based upon understanding of the issue, the authors proposed a simple mathematical model, which contains two reasonable constraints. The relation of the ''extreme'' intensity with both duration and region (EIDR) is derived. With the prescribed baseline extreme intensities, the authors calculate the relative intensities with the data. Through comparison among different time periods and spatial sizes, one can identify the event that is most extreme, with its starting time, duration, and geographic region being determined. Procedures for monitoring the extreme event are provided. As an example, the extreme event contained in the 1991 persistent heavy rainfall over east China is detected.

1. Introduction

It is generally believed that with global warming, weather and climate extremes tend to occur more frequently than ever (e.g., Karl and Knight 1998; Suppiah and Hennessy 1998; Meehl et al. 2000; Easterling et al. 2000; Klein Tank and Können 2003; Schmidli and Frei 2005; Wang and Zhou 2005; Nandintsetseg et al. 2007; Allan and Soden 2008; Krishnamurthy et al. 2009; Rodrigo 2010; Teixeira and Satyamurty 2011; Groisman et al. 2012; Piccarreta et al. 2013; Villarini et al. 2013; Lu et al. 2014). However, there is still no final exclusive definition for the extremes. Methodologies and metrics are required to identify and monitor the extremes on time scales from daily to decadal (e.g., Klein Tank and Können 2003; Garrett and Müller 2008; Zolina et al. 2010; Lu et al. 2015; Guinard et al. 2015; Wasko and Sharma 2015; Wasko et al. 2016). Proposing proper monitoring and detection methods is essential to the better understanding of the formation mechanisms of the extreme events and is particularly important to the reliable assessment of the long-term changes in the extremes.

Karl et al. (1996) constructed the climate extremes index (CEI) with multiple quantities, attempting to

Corresponding author: Er Lu, elu@nuist.edu.cn

DOI: 10.1175/JCLI-D-17-0105.1

© 2017 American Meteorological Society. For information regarding reuse of this content and general copyright information, consult the AMS Copyright Policy (www.ametsoc.org/PUBSReuseLicenses).

Downloaded from http://journals.ametsoc.org/jcli/article-pdf/30/16/6123/4680886/jcli-d-17-0105_1.pdf by guest on 25 September 2020

indicate the overall extreme condition in the climate. In many previous studies, extremes were extracted from a single climate quantity (e.g., the precipitation) and for each of the observation stations or a specific region examined. With daily precipitation data, researchers mainly found the daily extremes (e.g., Karl and Knight 1998; Liebmann et al. 2001; Klein Tank and Können 2003; Gershunov and Cayan 2003; Zhai et al. 2005; Nandintsetseg et al. 2007; Zolina et al. 2009; Rodrigo 2010; Piccarreta et al. 2013; Benestad 2013).

An extreme event always appears over a certain region and maintains for a certain period of time. In order for a precipitation event to be extreme, the event should last for a long period of time and affect a wide region while maintaining a strong intensity. However, if the region is taken improperly as too wide and the time period is taken as too long, then the intensity of the precipitation averaged over the region and the time period would be too weak. Hence, we need to have a balance among the geographic region, the time period, and the averaged intensity, the three elements for describing the extreme event. The goal of the present study is to identify, from a temporal–spatial rainfall process, the geographic region and the time period of the extreme event.

As a first step toward the issue, Lu et al. (2015) developed a method to find the extreme from the precipitation of a single station (or a fixed area). The time period is identified so that the event over the period is most extreme, compared with other events that are over other time periods. They proposed a mathematical model that includes two reasonable constraints. One is that for the multiday process, in which the rainfalls of the days are bound together, in order to reflect the scale (or size) effect, the rainfall of a longer duration may require having a weaker averaged intensity. The other is that the rainfall of a longer duration should be more in the total amount.

Based on these constraints, Lu et al. (2015) established a sound relation, the relation of the ''extreme'' intensity with duration (EID), which prescribes the standard or baseline of the intensity (i.e., the minimum intensity that an event of a specific duration needs to reach in order for the event to be an extreme). The intensities of different time periods calculated from the data are then compared with the prescribed extreme intensities. With this, the starting time and duration, within the process, are extrapolated so that the event with this time period can be most extreme, compared with the events that are over other time periods.

The EID relation is for a temporal series. In this study, we first apply the principle to space, finding the extreme for a given time period in space. For the spatial distribution of the rainfall averaged over the time period, the relation of the extreme intensity with the geographic region (EIR) is established. Then, through combining the EID and EIR relations, the relation of the extreme intensity with both the duration and the region (EIDR) is obtained. With the baseline intensities prescribed by the EIDR relation, we can determine both the time period and the geographic region of the extreme event. Over the period and region, the event can be most extreme, compared with other events that are over other periods and/or over other regions.

The EIDR approach can be used for both detection from the historical data and monitoring of the present weather. Operational procedures are also provided in this study. For daily monitoring, we identify whether the extreme event has emerged or not until the present date. If it has emerged, then we determine when the event started and over which region the event was maintained. When the rainy season is over, we may detect over the entire season and find over which period and over which region the event is most extreme compared to the events that are over other periods and regions.

The approach of the EID is briefly described in section 2. In section 3, we apply the principle to space and establish the EIR relation. In section 4, we combine the EID and EIR relations and derive the EIDR relation, for comparing the events that are over different durations and regions. The operational procedures for the day-to-day monitoring and detection of the extreme event from both time and space are provided in section 5. A real example of the monitoring is presented in section 6. A summary and discussion are given in section 7.

The rainfall data used in section 6 to find the extreme event over east China during the warm season of 1991 were provided by the China National Center for Meteorological Information (http://data.cma.cn/data/detail/dataCode/SURF_CLI_CHN_PRE_DAY_GRID_0.5). The dataset is an analysis of the daily precipitation observed from 2472 stations over China, starting from 1961 and with a horizontal resolution of 0.5° × 0.5°.

2. The principle of the EID

For the precipitation of a fixed region (or a station), Lu et al. (2015) proposed a method to determine the time period of the extreme event. The simple mathematical model they used contains the following two constraints.

For the precipitation averaged over a fixed area S, the first constraint is that with the increase in duration T, the precipitation intensity of the extreme I_S should decrease, and this can be expressed as $dI_S/dT < 0$. The second constraint is that with the increase in duration,

Downloaded from http://journals.ametsoc.org/jcli/article-pdf/30/16/6123/4680886/jcli-d-17-0105_1.pdf by guest on 25 September 2020

though the intensity decreases, the rainfall total of the extreme (i.e., the product of the intensity and duration) should increase, and this can be expressed as $d(I_S T)/dT > 0$.

Combining these two relations yields $0 < a < 1$, where a satisfies $d(\ln I_S) = -ad(\ln T)$. Our purpose is to prescribe the $I_S(T)$, that is, to express the extreme intensity I_S in terms of the duration T. In other words, the I_S is the quantity we need to obtain, not a quantity we already have.

As pointed out in Lu et al. (2015), in order to better obey the above two constraints, the parameter a (in the relation $0 < a < 1$) should not be too close to 0 and not be too close to 1. We may mathematically treat the parameter a as a constant, and thus the value of 0.5 is an appropriate choice for the parameter.

Integrating the equation $d(\ln I_S) = -ad(\ln T)$ yields

$$I_S(T) = I_S(1) \times T^{-a}, \tag{1}$$

where $I_S(1)$ is the extreme intensity with the duration T being 1 (unit). It is a constant and can be determined with a threshold.

Equation (1) establishes the relation of the EID. With this baseline extreme intensity, the precipitation intensities of different durations can be compared. Lu et al. (2015) defined the ''relative intensity,'' which is the ratio of the observed precipitation intensity averaged over duration T to the baseline intensity $I_S(T)$, or simply the ratio of the observed intensity to the factor T^{-a} in Eq. (1). In the day-to-day monitoring or detections, with the finding of the maximum among the relative intensities, the time period (i.e., the starting time and duration) of the extreme event can be identified.

3. Applying the EID approach to space

The principle (i.e., the two constraints) of the EID can also be applied to space for the precipitation of a fixed time period. Thus, from the spatial distribution of the precipitation, we can find over which geographic region the event is most extreme.

For a specific duration T, the first constraint is that with the increase in the area S of the geographic region, the extreme intensity I_T should decrease, and this can be expressed as $dI_T/dS < 0$. The second constraint is that with the increase in the area, though with a decrease in intensity, the total rainfall amount of the extreme over the region (i.e., the product of the intensity and area) should increase, and this can be expressed as $d(I_T S)/dS > 0$.

Combining the two constraints yields $0 < b < 1$, where b satisfies $d(\ln I_T) = -bd(\ln S)$. Integrating the equation yields

$$I_T(S) = I_T(1) \times S^{-b}, \tag{2}$$

where $I_T(1)$ is the extreme intensity with the area S being 1 (unit). Equation (2) is the relation of the EIR.

Similar to Lu et al. (2015), with the baseline intensity prescribed in Eq. (2), the relative intensity is defined as $R(S) \equiv \overline{I}(S)/I_T(S)$, where $\overline{I}(S)$ is the observed precipitation averaged over the area S. Since $I_T(1)$ is a constant, we omit it and write the relative intensity as $R(S) = \overline{I}(S) \times S^b$.

Figure 1a shows conceptually an example of finding the geographic region of the event that is most extreme. The precipitation here is an average over a certain time period. Through extrapolating among a given simple rainfall matrix, we obtain the values of the precipitation at each of the grids and then plot the contours of the rainfall. The area enclosed by a contour is calculated with the number of the grids contained, and the mean rainfall intensity over the region is calculated with the values of the rainfall over the grids. With the relative intensity defined above, the relative intensities of the different events, characterized by the regions enclosed by the different contours, are compared.

Figure 1b illustrates how the relative intensity R varies with the value of the contour k. The event with the region enclosed by the contour of 10 units is maximal in relative intensity and thus is the most extreme event. The geographic region of this contour is highlighted in Fig. 1a. Figure 1b also shows that the events with the regions enclosed by the contours close to this one (i.e., the contours of 9 and 11 units, or even the contours of 8 and 12 units) are also large in their relative intensities. So, it would not be erroneous to treat the events over the regions of these contours as the extremes. However, as indicated in Fig. 1b, relative intensity decreases sharply when the area of the contour becomes very small or very large. Therefore, it would be inappropriate to treat the events over these very small or very large regions (e.g., the one enclosed by the contour of 16 or 2 units) as the extreme events.

4. Comparing the events that are over different durations and regions

The $I_S(T)$ in Eq. (1) describes how the extreme intensity of a fixed region (or station) varies with the duration, whereas the $I_T(S)$ in Eq. (2) describes how the extreme intensity of a specific duration varies with the area. They are both one-dimensional. Here, in the context of the two-dimensional variation (i.e., the variation of the extreme intensity I_e with both the duration and the area), they can be rewritten as

Downloaded from http://journals.ametsoc.org/jcli/article-pdf/30/16/6123/4680886/jcli-d-17-0105_1.pdf by guest on 25 September 2020

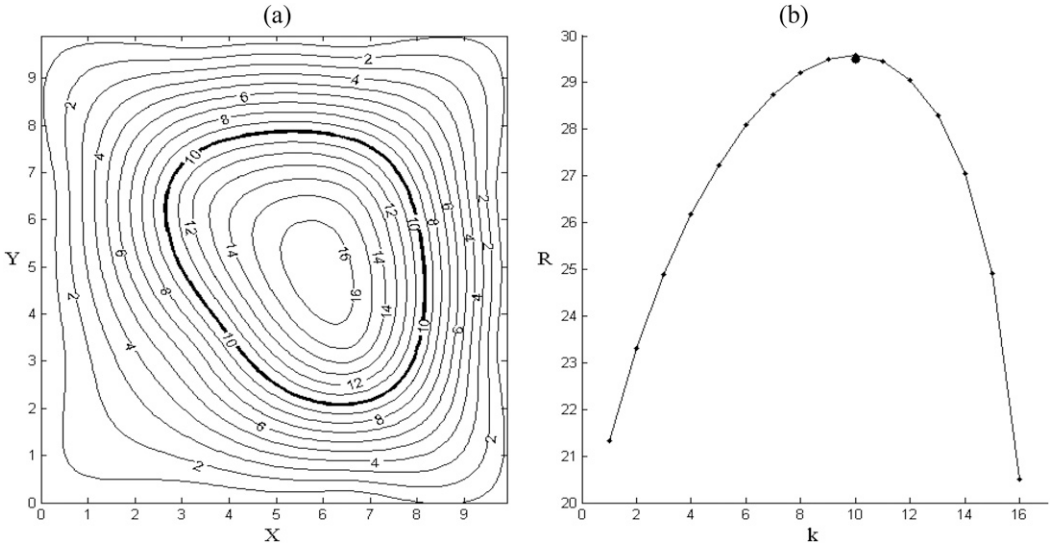

FIG. 1. A conceptual example of determining the geographic region of the extreme, from the spatial distribution of the precipitation that is averaged over a certain time period. (a) The contours indicate the distribution of the rainfall over the domain, in which X and Y both range from 0 to 10, with a resolution of 0.1 (appropriate units can be given to the rainfall and the distance). The contours are obtained through the extrapolations among a given 4×4 matrix, with the four rows of the matrix being from top to bottom (0,0,0,0), (0,15,14,0), (0,7,12,0), and (0,0,0,0). The contours finally range from 0, which is along the four borders of the domain, to 16, which is the innermost contour. (b) The curve presents the value of the relative intensity R corresponding to the value of each of the contours k in (a).

$$I_e(T,S) = I_e(1,S) \times T^{-a} \tag{3}$$

and

$$I_e(T,S) = I_e(T,1) \times S^{-b}. \tag{4}$$

In Eq. (3), let $S = 1$, and then we obtain $I_e(T, 1) = I_e(1, 1) \times T^{-a}$. Substituting this into Eq. (4) yields

$$I_e(T,S) = I_e(1,1) \times T^{-a} \times S^{-b}, \tag{5}$$

where $I_e(1, 1)$ is the extreme intensity of the event that has the shortest duration and the smallest region, limited by the temporal and spatial resolutions (i.e., the units of the duration and area). It can be determined with a threshold (say, the top 5%) or simply be given. Equation (5) establishes the relation of the EIDR.

With this baseline intensity, the relative intensity is defined as

$$R(T,S) \equiv \overline{I}(T,S)/I_e(T,S), \tag{6}$$

where $\overline{I}(T, S)$ is the intensity of the observed precipitation, averaged over a time period with duration T and over a geographic region S. Substituting Eq. (5) into Eq. (6) yields

$$R(T,S) = \overline{I}(T,S) \times (T^a \times S^b), \tag{7}$$

where we have omitted the factor $I_e(1, 1)$, which is a constant.

As analyzed in Lu et al. (2015) and in section 2 of this study, the parameter a can be assigned a moderate value between 0 and 1, and thus $a = 0.5$. Through giving values to the (initial) extreme intensities of different durations based on various thresholds, it was demonstrated that the parameter a varies slightly around 0.5 (Lu et al. 2015). Zhang et al. (2013) used certain thresholds to define the extreme intensities and examined the relationship among the intensities. Their results also indicate that the reference extreme precipitation intensity is inversely proportional to the square root of the duration. It was illustrated, in Fig. 3 of Lu et al. (2015), that for the events that are significantly extreme, the identifications of the extreme events are not sensitive to the small variations of the parameter a (e.g., from 0.4 to 0.6). Similarly, we also let $b = 0.5$ (e.g., Hutchinson 1998).

For general operational monitoring and detection, the formula of the relative intensity can thus be written as

$$R(T,S) = \overline{I}(T,S) \times (T \times S)^{0.5}. \tag{8}$$

Equation (8) suggests that for a temporal–spatial rainfall event, a longer duration T, a wider region S, and a stronger averaged intensity $\overline{I}$ can all contribute to make the event gain a larger relative intensity and thus make it easier to be extreme. What is interesting in

Downloaded from http://journals.ametsoc.org/jcli/article-pdf/30/16/6123/4680886/jcli-d-17-0105_1.pdf by guest on 25 September 2020

Eq. (8) is the manner in which the averaged intensity $\overline{I}$ "stays" with the duration T and the region S. Instead of staying with the T and S themselves, the averaged intensity $\overline{I}$ stays with their square roots, that is, $(T \times S)^{0.5}$.

For a rainfall event, it may sometimes be hard for all of the three elements (i.e., the duration, region, and averaged intensity) to be large in their values. We can use Eq. (8) to assess the overall strength of the event. Those events that last for short periods of time and/or occur over small areas (e.g., the convective thunderstorms), based on Eq. (8), may still be extreme, as long as their relative intensities are sufficiently large.

5. Operational procedures for the temporal–spatial monitoring of extreme event

Using the concept of relative intensity, we are able to monitor and detect the extreme rainfall event, simultaneously from both time and space. The monitoring is performed routinely for each day. The operational procedures are described as follows:

1) When rainfall has occurred for some time and we feel there is a need, we may start the monitoring. For example, we start the monitoring beginning on 1 April and end the monitoring on 31 October. The monitoring is performed for every "present day," and we denote the date of the present day as "day n."
2) For a given present day n, we consider all the time periods, including the present day itself and all the periods that end on the present day but start 1, 2, 3, . . . , (up to 30, 60, or 90) days prior to the present day. We denote the start date as "day m." So, we examine all the time periods that start from day m and end on day n.
3) For a given time period m, n, we average the precipitation over the period and then plot the spatial distribution of the mean rainfall. Similar to Fig. 1a, all the regions enclosed by the contours are considered. We denote the value of a contour as k. It may take the values of, for example, 1, 2, . . . , 50 (depending on unit and the need).
4) We calculate the relative intensity for the region of each contour, using Eq. (8). The relative intensity is a function of the contour k as well as the time period m, n and thus can be denoted as $R(m, n, k)$.
5) Among all the contours (say, $k = 1, 2, \ldots, 50$), similar to Fig. 1a, we find the maximum from the values of the relative intensity R, which can be expressed as

$$R_1(m,n,K) = \operatorname*{Max}_k [R(m,n,k)], \tag{9}$$

where K is the value of the k with which the relative intensity R gains its maximum. The K here is for the time period (m, n). It is thus a function of m and n and is denoted as $K(m, n)$.

6) With the variation of the starting date m, say, from 0 (actually the present day itself), 1, 2, 3, . . . , up to 90, we find the maximum from the values of the relative intensity R_1, which can be expressed as

$$R_2(M,n,K) = \operatorname*{Max}_m [R_1(m,n,K)], \tag{10}$$

where M is the value of the m with which the relative intensity R_1 gains its maximum. The M here corresponds to the present day n. It is thus a function of n and can be denoted as $M(n)$. The K is then denoted as $K[M(n), n]$.

With this procedure, we can identify (until the present day n) whether an extreme event has emerged or not. If it has emerged, then the starting date of the event (and thus the duration) and the geographic region of the event are determined.

Note that we need to have a standard (or threshold) to define the intensity of the extreme event, and this can be specified by the factor $I_e(1, 1)$; for simplicity, we have omitted this factor in Eq. (7).

7) With the moving of the present day n, for example, from 1 to 2 June, we repeat the above monitoring procedures and determine whether an extreme event has emerged or not until this new present day n. Through repeating this procedure, we perform the day-to-day monitoring of the extreme rainfall event.
8) When the rainy season is over (e.g., after 31 October, as mentioned above), we stop the monitoring. Then, we can go back to find the maximum from the values of the relative intensity R_2, and this can be expressed as

$$R_3(M,N,K) = \operatorname*{Max}_n [R_2(M,n,K)], \tag{11}$$

where N is the value of the n with which the relative intensity R_2 gains its maximum. With this present day N being determined, the corresponding starting date M and the contour K can also be determined. They are $M(N)$ and $K[M(N), N]$, respectively.

Through this detection procedure, we can find the most extreme rainfall event during the rainy season. It starts from day $M(N)$ and ends on day N. Its geographic region is the area enclosed by the contour $K[M(N), N]$.

6. A real example of the operational monitoring

The heavy rainfall that occurred during May–July 1991 over the Yangtze–Huaihe River basin caused tremendous social and economic impacts. In previous studies (e.g., Lu et al. 1994, 1998; Lu and Ding 1997a,b), the abnormalities in the atmospheric circulation were

Downloaded from http://journals.ametsoc.org/jcli/article-pdf/30/16/6123/4680886/jcli-d-17-0105_1.pdf by guest on 25 September 2020

TABLE 1. The record of the day-to-day monitoring for the maximal relative intensity $R_1(m, n, K)$ (mm day^{-1}), which is spatially sought among all the contours k of each time period m, n. This is a portion of the full table, with the aim to display the $R_3(M, N, K)$ (=391.6 mm day^{-1}), the maximal relative intensity during the entire rainy season (this value is shown in boldface text). The full table records the daily monitoring that starts on 1 May and ends on 31 Jul. For each present day n, we consider all the time periods that end on n but start from m, a prior date, which can be up to 3 months before the present day.

Starting date (m)	Present day (n)								
	15 Jul	14 Jul	13 Jul	12 Jul	11 Jul	10 Jul	9 Jul	8 Jul	7 Jul
26 Jun	323.04	325.84	333.69	342.06	346.51	320.23	308.89	272.71	257.87
27 Jun	331.27	334.6	343.19	352.41	357.7	331.28	320.35	283.63	269.11
28 Jun	340.22	344.17	353.61	363.82	370.11	343.63	333.27	296.05	282.05
29 Jun	349.81	354.48	364.93	376.3	383.79	357.35	347.75	310.14	296.91
30 Jun	352.89	359.37	370.82	383.33	**391.6**	365.32	355.81	318.93	306.61
1 Jul	349.15	356.67	369.15	382.81	391.04	363.85	354.24	318.26	305.31
2 Jul	324.47	330.99	343.45	357.36	365.03	336.6	327.53	288.08	275.02
3 Jul	320.29	326.77	340.17	355.4	365.64	334.78	327.37	283.13	271.27
4 Jul	282.35	288.2	300.97	315.83	321.84	289.47	282.88	243.83	234.23

analyzed for the period of the three months or the major three rainfall episodes during the season. Here, using the operational temporal–spatial monitoring procedures described in section 5, we detect the event that is most extreme during the season in both space and time and determine the starting and ending dates as well as the geographic region of the event.

We start the daily monitoring beginning on 1 May and end it on 31 July. For each present day n, we consider all the time periods that end on the present day but start from a prior date m, which can be up to 90 days before the present day. Again, for each time period, we plot the contours k of the rainfall averaged over the period and calculate the relative intensity $R(m, n, k)$, which takes into account both the duration of the period as well as the area of the contours. The maximal relative intensity is sought for the period from the values of the relative intensity of all the contours. With the day-to-day monitoring, we obtain the event (i.e., its starting and ending dates and geographic region) that is most extreme until the present day.

We use a two-dimensional table to record the results of the day-to-day monitoring for all the time periods m, n. The values in the table are the relative intensity $R_1(m, n, K)$, which has been spatially sought among all the contours k for each time period m, n. Table 1 is a portion of the record, which focuses on the $R_3(M, N, K)$, the maximal relative intensity of the entire rainy season. The event that is most extreme over the 3 months is the one that starts on 30 June, which is the M, and ends on 11 July, which is the N. The maximal relative intensity R_3 is 391.60 mm day^{-1} (the boldface text in the table). It is shown from the table that for the event that starts on 1 July and ends on 11 July, the relative intensity is also sufficiently large (391.04 mm day^{-1}). Hence, it is acceptable if we take the starting time of the event to be one day later (i.e., from 30 June to 1 July).

Figure 2 displays the contours of the rainfall averaged over 30 June–11 July, the time period of the identified most extreme event. The area enclosed by the contour of 31 mm day^{-1} (thick line) is the geographic region of the extreme event. The relative intensity over this region is maximal (391.60 mm day^{-1}) during the entire rainy season. As expected, this region is in the form of a band, along the Yangtze–Huaihe River basin.

Figure 3 presents the relative intensity corresponding to each of the contours in Fig. 2. In addition to the contour of 31 mm day^{-1}, which is maximal in relative intensity, the contour of 32 mm day^{-1} also possesses a large relative intensity. So, it would not be erroneous to treat the area of this contour as the geographic region of the extreme event also. However, for those contours that enclose a very large or very small area, the relative intensities are much smaller, and thus the corresponding events would not be that extreme.

Figure 4 shows the daily rainfall averaged over the region of the most extreme event (i.e., the region enclosed by contour 31 in Fig. 2). The identified time period of this most extreme event is from 30 June to 11 July (red bars). By intuition, daily rains are relatively large during these consecutive days, and they can well reflect the scale (or size) effect. The rain during the period from 18 May to 15 June is relatively small on average, although it lasts for a longer time period. Since there is a large gap between this period and the period identified (30 June–11 July), the event with these two periods combined (i.e., for the long period from 18 May to 11 July) would not be very extreme, compared with the latter period alone.

7. Summary and discussion

Heavy rainfall events occur frequently in China. To stress the severity of an event, it is generally described

Downloaded from http://journals.ametsoc.org/jcli/article-pdf/30/16/6123/4680886/jcli-d-17-0105_1.pdf by guest on 25 September 2020

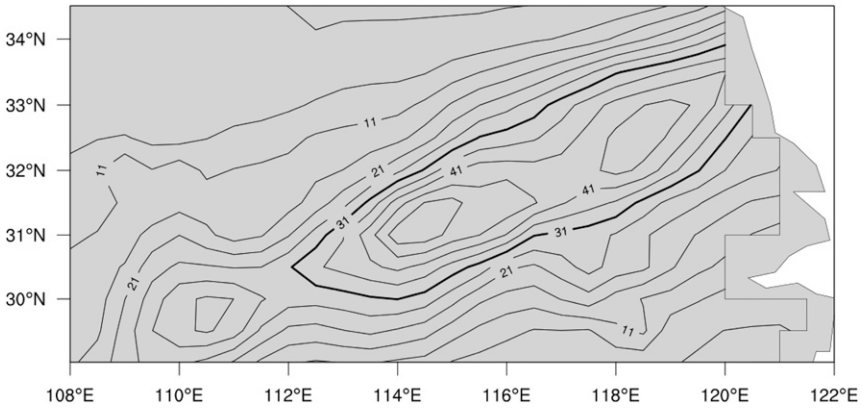

FIG. 2. The contours of the rainfall averaged over the period from 30 Jun (M) to 11 Jul (N), the period of the detected most extreme event during the rainy season. The contour corresponding to the maximal relative intensity $R_3(M, N, K)$ (= 391.6 mm day^{-1}), with its value K being 31 mm day^{-1}, is thickened.

that "the event lasted for a long period of time, affected a wide region, and maintained a strong intensity." However, if the time is taken as too long and the area is taken as too wide, then the intensity of the rainfall averaged over the area and the time period may not be that strong (relative to the area and duration). Hence, we need to have a balance among the geographic region, the time period, and the averaged intensity.

As a first step for the issue of considering both the time period and the geographic region, Lu et al. (2015) focused on the temporal series of the rainfall of a fixed area (or a station), finding extremes among the different time periods (different starting times and/or durations). The principle for constructing the relation of the extreme intensity with duration (EID) is that with the increase in duration the baseline intensity decreases but the corresponding rainfall amount increases. These constraints actually reflect the scale (or size) effect of the bound multiday (long duration) events. By using the obtained baseline extreme intensities, events of different time periods (different starting times and/or durations) calculated from the data can be compared with each other. According to this, short-duration events may also be extreme, as long as they can have, relatively, very strong intensities.

In previous studies, as suggested in Junker et al. (2008), the conventional understanding considers the starting and ending times as well as the breaks in the rainfall.

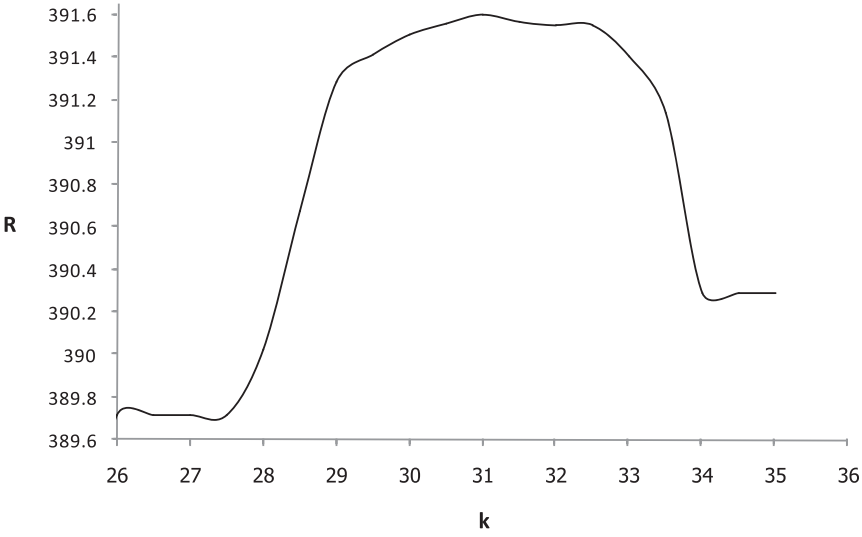

FIG. 3. The variation of the relative intensity $R(M, N, k)$ (mm day^{-1}) with the value of contour k (mm day^{-1}). The contours of the rainfall averaged over the period M, N are displayed in Fig. 2.

Downloaded from http://journals.ametsoc.org/jcli/article-pdf/30/16/6123/4680886/jcli-d-17-0105_1.pdf by guest on 25 September 2020

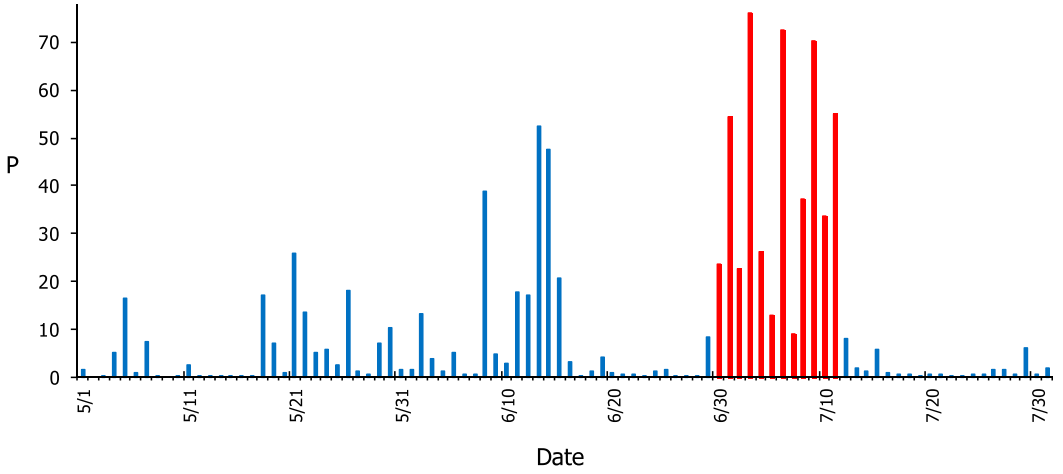

FIG. 4. The daily rainfall (P; mm day^{-1}) averaged over the identified region, the one enclosed by the contour K (=31 mm day^{-1}) in Fig. 2. The red bars are for the period from 30 Jun (M) to 11 Jul (N), the detected period of the most extreme event during the rainy season.

These studies find difficulty in dealing with the multiday rainfall process when it comes as a result of several consecutive storms with breaks between them. In Lu et al. (2015), their Figs. 1e and 1f illustrated that these are no longer problems for the EID method. The storms in the multiday rainfall process may be caused by different synoptic systems and due to the movements and evolution of different precipitating systems. Nevertheless, these storms all contribute to affect the local hydrological condition and help form an extreme precipitation event. For monitoring, our goal is to identify whether these persistent storms can be extreme as a result.

What is interesting in the EID method is that the relative intensity is linked to the square root of the duration, not the duration itself. Although this relationship is derived from a simple theoretical model, it can be understood and verified from historical data. Lu et al. (2015) estimated the value of the parameter a in their Fig. 5, through giving ''initial'' extreme intensities of different durations with various thresholds for the observed precipitation data. Their results showed that the estimated values of the parameter were all around 0.5. Using historical data and certain thresholds for defining the extreme intensities, Zhang et al. (2013) also found that extreme precipitation intensity is nearly inversely proportional to the square root of the rainfall duration. Note that in the above estimations and verifications, we need to provide values for the intensities of different durations based on certain thresholds (we thus call them the initially defined intensities of different durations). However, the extreme intensity is the quantity we need to determine (our task), not a quantity for which we already have values.

The principle of the EID, that is, the consideration of the scale (or size) effect, can also be applied to space to find the rainfall event (of a time period) that is most extreme among the regions that are different in size. For instance, we may determine whether the event in the size of a village, a county, or a province can be most extreme. It is reasonable to hypothesize that with the increase in the area (size), the baseline intensity of the extreme decreases, while the rainfall total over the area increases. Based on the constraints, the relation of the extreme intensity with geographic region (EIR) was established. With the defined relative intensities, the events that are over different locations and/or in different sizes can be compared, and the event that is spatially most extreme can thus be found.

Through combining the EID and EIR relations, we finally obtained the relation of the extreme intensity with both the duration and the region (EIDR). With the prescribed baseline intensities of the extremes, the events that are over different time periods and/or over different geographical regions can be compared. So, finally, we would be able to tell over which period and over which region the intensity averaged over them is the strongest, when compared with the events that are over other time periods and over other geographic domains, and thus the event over this period and region can best be determined as extreme. [The unit of precipitation, which is generally mm day^{-1}, can be converted into m^3 (m^2 day)$^{-1}$.] The issue here is to find the time period (with unit of day) and the area (with unit of m^2) so that the volume (with unit of m^3) of the rainfall (water) over the period and the region can relatively (relative to the duration and area) be the largest.

Downloaded from http://journals.ametsoc.org/jcli/article-pdf/30/16/6123/4680886/jcli-d-17-0105_1.pdf by guest on 25 September 2020

Based on the EIDR approach, operational procedures for the temporal–spatial monitoring of an extreme event are provided step by step in this study. For each "present day," the monitoring is performed for all the periods that end on the present day but start from each of the earlier dates. For a given time period, we plot the spatial distribution of the rainfall averaged over the period. The relative intensities are compared among all of the regions enclosed by the different contours. Note that since the relative intensities are computed with both the period and the area being taken into account, the maximal relative intensity spatially sought from the contours can be compared among different periods. So, finally, for each present day, we can determine over which period, until the present day, the rainfall event sought is the most extreme one. With the day-to-day monitoring across the entire rainy season, we can obtain the relative intensity that is temporally maximal over the season and detect the most extreme rainfall event of the season, with its starting time, duration, and geographic region being determined.

The temporal–spatial monitoring is performed with a real example for the persistent heavy rainfall over east China during May–July 1991. With this EIDR approach, an operational system for the temporal–spatial monitoring of the extreme rainfall event is under construction in the National Climate Center of China. In the programming for the two-dimensional spatial pattern, the algorithm for convex hulls (e.g., Andrew 1979; Brown 1979; Chazelle 1993) is being utilized. The present work is performed in the Eulerian space and does not track the storm center. As an extension, the Lagrangian space (e.g., May and Julien 1998) will be considered in the operational system.

Acknowledgments. This study was supported jointly by the China Special Fund for Meteorological Research in the Public Interest (major projects) (Grant GYHY201506001, Er Lu), the Science and Technology Bureau of Liaoning Province (Grant 2015103038, Chunyu Zhao), the National Climate Center of China (Grant CMAHX20160502, Dianxiu Ye), the National Natural Science Foundation of China (Grant 41275092, Er Lu), the Center for Weather and Climate Extremes (CWCE) at Nanjing University of Information Science and Technology, and the Priority Academic Program Development of Jiangsu Higher Education Institutions (PAPD). The precipitation data used were provided by the China National Center for Meteorological Information.

REFERENCES

Allan, R. P., and B. J. Soden, 2008: Atmospheric warming and the amplification of precipitation extremes. *Science*, **321**, 1481–1484, doi:10.1126/science.1160787.

Andrew, A. M., 1979: Another efficient algorithm for convex hulls in two dimensions. *Inf. Process. Lett.*, **9**, 216–219, doi:10.1016/0020-0190(79)90072-3.

Benestad, R. E., 2013: Association between trends in daily rainfall percentiles and the global mean temperature. *J. Geophys. Res. Atmos.*, **118**, 10 802–10 810, doi:10.1002/jgrd.50814.

Brown, K. Q., 1979: Voronoi diagrams from convex hulls. *Inf. Process. Lett.*, **9**, 223–228, doi:10.1016/0020-0190(79)90074-7.

Chazelle, B., 1993: An optional convex hull algorithm in any fixed dimension. *Discrete Comput. Geom.*, **10**, 377–409, doi:10.1007/BF02573985.

Easterling, D. R., J. L. Evans, P. Ya. Groisman, T. R. Karl, K. E. Kunkel, and P. Ambenje, 2000: Observed variability and trends in extreme climate events: A brief review. *Bull. Amer. Meteor. Soc.*, **81**, 417–425, doi:10.1175/1520-0477(2000)081<0417:OVATIE>2.3.CO;2.

Garrett, C., and P. Müller, 2008: Extreme events. *Bull. Amer. Meteor. Soc.*, **89**, 1733, doi:10.1175/2008BAMS2566.1.

Gershunov, A., and D. R. Cayan, 2003: Heavy daily precipitation frequency over the contiguous United States: Sources of climatic variability and seasonal predictability. *J. Climate*, **16**, 2752–2765, doi:10.1175/1520-0442(2003)016<2752:HDPFOT>2.0.CO;2.

Groisman, P. Ya., R. W. Knight, and T. R. Karl, 2012: Changes in intense precipitation over the central United States. *J. Hydrometeor.*, **13**, 47–66, doi:10.1175/JHM-D-11-039.1.

Guinard, K., A. Mailhot, and D. Caya, 2015: Projected changes in characteristics of precipitation spatial structures over North America. *Int. J. Climatol.*, **35**, 596–612, doi:10.1002/joc.4006.

Hutchinson, M. F., 1998: Interpolation of rainfall data with Thin Plate Smoothing Splines—Part I: Two dimensional smoothing of data with short range correlation. *J. Geogr. Inf. Decis. Anal.*, **2**, 139–151.

Karl, T. R., and R. W. Knight, 1998: Secular trends of precipitation amount, frequency, and intensity in the United States. *Bull. Amer. Meteor. Soc.*, **79**, 231–241, doi:10.1175/1520-0477(1998)079<0231:STOPAF>2.0.CO;2.

——, ——, D. R. Easterling, and R. G. Quayle, 1996: Indices of climate change for the United States. *Bull. Amer. Meteor. Soc.*, **77**, 279–292, doi:10.1175/1520-0477(1996)077<0279:IOCCFT>2.0.CO;2.

Klein Tank, A. M. G., and G. P. Können, 2003: Trends in indices of daily temperature and precipitation extremes in Europe, 1946–99. *J. Climate*, **16**, 3665–3680, doi:10.1175/1520-0442(2003)016<3665:TIIODT>2.0.CO;2.

Krishnamurthy, C. K. B., U. Lall, and H. H. Kwon, 2009: Changing frequency and intensity of rainfall extremes over India from 1951 to 2003. *J. Climate*, **22**, 4737–4746, doi:10.1175/2009JCLI2896.1.

Liebmann, B., C. Jones, and L. M. V. Carvalho, 2001: Interannual variability of daily extreme precipitation events in the state of São Paulo, Brazil. *J. Climate*, **14**, 208–218, doi:10.1175/1520-0442(2001)014<0208:IVODEP>2.0.CO;2.

Lu, E., and Y. Ding, 1997a: Low frequency oscillation in East Asia during the 1991 excessively heavy rain over the Changjiang-Huaihe River basin (in Chinese). *Acta Meteor. Sin.*, **11**, 12–22.

——, and ——, 1997b: Analysis of summer monsoon activity during the 1991 excessively torrential rain over the Changjiang-Huaihe River basin. *J. Appl. Meteor. Sci.*, **8**, 316–324.

——, ——, and Y. Li, 1994: Isentropic potential vorticity analysis and cold air activity during the period of excessively heavy rain over the Changjiang-Huaihe River basin in 1991 (in Chinese). *J. Appl. Meteor. Sci.*, **5**, 266–274.

——, ——, M. Murakami, and K. Takahashi, 1998: Nature of precipitation and activity of cumulus convection during the

Downloaded from http://journals.ametsoc.org/jcli/article-pdf/30/16/6123/4680886/jcli-d-17-0105_1.pdf by guest on 25 September 2020

1991 meiyu season of the Changjiang-Huaihe River basin. *Acta Meteor. Sin.*, **12**, 75–91.

——, and Coauthors, 2014: Changes of summer precipitation in China: The dominance of frequency and intensity and linkage with changes in moisture and air temperature. *J. Geophys. Res. Atmos.*, **119**, 12 575–12 587, doi:10.1002/2014JD022456.

——, and Coauthors, 2015: Determining starting time and duration of extreme precipitation events based on intensity. *Climate Res.*, **63**, 31–41, doi:10.3354/cr01280.

May, D., and J. Julien, 1998: Eulerian and Lagrangian correlation structures of convective rainstorms. *Water Resour. Res.*, **34**, 2671–2683, doi:10.1029/98WR01531.

Meehl, G. A., F. Zwiers, J. Evans, T. Knutson, L. Mearns, and P. Whetton, 2000: Trends in extreme weather and climate events: Issues related to modeling extremes in projections of future climate change. *Bull. Amer. Meteor. Soc.*, **81**, 427–436, doi:10.1175/1520-0477(2000)081<0427:TIEWAC>2.3.CO;2.

Nandintsetseg, B., J. S. Greene, and C. E. Goulden, 2007: Trends in extreme daily precipitation and temperature near lake Hövsgöl, Mongolia. *Int. J. Climatol.*, **27**, 341–347, doi:10.1002/joc.1404.

Piccarreta, M., A. Pasini, D. Capolongo, and M. Lazzari, 2013: Changes in daily precipitation extremes in the Mediterranean from 1951 to 2010: The Basilicata region, southern Italy. *Int. J. Climatol.*, **33**, 3229–3248, doi:10.1002/joc.3670.

Rodrigo, F. S., 2010: Changes in the probability of extreme daily precipitation observed from 1951 to 2002 in the Iberian Peninsula. *Int. J. Climatol.*, **30**, 1512–1525, doi:10.1002/joc.1987.

Schmidli, J., and C. Frei, 2005: Trends of heavy precipitation and wet and dry spells in Switzerland during the 20th century. *Int. J. Climatol.*, **25**, 753–771, doi:10.1002/joc.1179.

Suppiah, R., and K. J. Hennessy, 1998: Trends in total rainfall, heavy rain events and number of dry days in Australia, 1910–1990. *Int. J. Climatol.*, **18**, 1141–1164, doi:10.1002/(SICI)1097-0088(199808)18:10<1141::AID-JOC286>3.0.CO;2-P.

Teixeira, M. S., and P. Satyamurty, 2011: Trends in the frequency of intense precipitation events in southern and southeastern Brazil during 1960–2004. *J. Climate*, **24**, 1913–1921, doi:10.1175/2011JCLI3511.1.

Villarini, G., J. A. Smith, and G. A. Vecchi, 2013: Changing frequency of heavy rainfall over the central United States. *J. Climate*, **26**, 351–357, doi:10.1175/JCLI-D-12-00043.1.

Wang, Y., and L. Zhou, 2005: Observed trends in extreme precipitation events in China during 1961–2001 and the associated changes in large-scale circulation. *Geophys. Res. Lett.*, **32**, L09707, doi:10.1029/2005GL022574.

Wasko, C., and A. Sharma, 2015: Steeper temporal distribution of rain intensity at higher temperatures within Australian storms. *Nat. Geosci.*, **8**, 527–529, doi:10.1038/ngeo2456.

——, ——, and S. Westra, 2016: Reduced spatial extent of extreme storms at higher temperatures. *Geophys. Res. Lett.*, **43**, 4026–4032, doi:10.1002/2016GL068509.

Zhai, P., X. Zhang, H. Wan, and X. Pan, 2005: Trends in total precipitation and frequency of daily precipitation extremes over China. *J. Climate*, **18**, 1096–1108, doi:10.1175/JCLI-3318.1.

Zhang, H., K. Fraedrich, X. Zhu, R. Blender, and L. Zhang, 2013: World's greatest observed point rainfalls: Jennings (1950) scaling law. *J. Hydrometeor.*, **14**, 1952–1957, doi:10.1175/JHM-D-13-074.1.

Zolina, O., C. Simmer, K. Belyaev, A. Kapala, and S. Gulev, 2009: Improving estimates of heavy and extreme precipitation using daily records from European rain gauges. *J. Hydrometeor.*, **10**, 701–716, doi:10.1175/2008JHM1055.1.

——, V. Detemmerman, and K. E. Trenberth, 2010: Improving the accuracy of estimation of climate extremes. *Eos, Trans. Amer. Geophys. Union*, **91**, 506, doi:10.1029/2010EO510013.

Downloaded from http://journals.ametsoc.org/jcli/article-pdf/30/16/6123/4680886/jcli-d-17-0105_1.pdf by guest on 25 September 2020